Hindawi
Geofluids
Volume 2023, Article ID 1181284, 12 pages
https://doi.org/10.1155/2023/1181284

Research Article

Risk Assessment of Water and Sand Inrush in Mining under Thick Loose Layer Based on Comprehensive Weight-Cloud Model

Wenquan Zhang,[1,2] **Xintao Wu**,[1,2] **Xunan Wu**,[1,2] **Yu Lei**,[1,2] **Jianli Shao**,[1,2] **and Zaiyong Wang**[1,2]

[1]*College of Energy and Mining Engineering, Shandong University of Science and Technology, Qingdao 266590, China*
[2]*State Key Laboratory of Strata Intelligent Control and Green Mining Co-founded by Shandong Province and the Ministry of Science and Technology, Qingdao 266590, China*

Correspondence should be addressed to Wenquan Zhang; wenquanzhang415@163.com

Received 15 July 2021; Revised 29 April 2022; Accepted 27 May 2022; Published 13 April 2023

Academic Editor: Andrea Brogi

Many deep mining mines in southwestern Shandong Province of China are covered with thick loose layers. When mining near the loose layers, there is a risk of water and sand inrush, which threatens the personal safety of miners. The prediction of sudden water and sand inrush is difficult due to the comprehensive influence of many factors, and the influencing factors are fuzzy and random. To solve this problem, in this paper, a new risk assessment method of water and sand inrush based on comprehensive weight and cloud model was proposed. Seven factors are selected as indexes: the aquifer thickness, the thickness ratio of sand layer to clay layer, the thickness of bottom clay layer, the coal seam thickness, the percentage of core recovery, the geological structure, and the bedrock thickness. The assessment index system is established, and the index is divided into three grades. A comprehensive weighting method, which combines analytic hierarchy process (AHP), entropy weight method (EWM), and minimum entropy principle, is used to reasonably assign the weight of index. Based on the cloud generator equation, the membership function is obtained. The assessment result of the assessment object is obtained by combining the membership degree and the weight of index. The comprehensive weight-cloud model assessment method is applied to the risk assessment of water and sand inrush in the 6311-2 working face in the sixth mining area of Baodian Coal Mine. According to the assessment results, the following conclusions can be drawn: (1) the bedrock thickness and the coal seam thickness are the main factors of water and sand inrush under loose layer mining; (2) the assessment results obtained by the comprehensive weight-cloud model method are consistent with the actual situation. The assessment method can provide scientific reference for the safe mining under the thick loose layer in the deep mines of southwest Shandong.

1. Introduction

Water and sand inrush is a kind of mine geological disaster that water and sand mixed fluid with high sand content bursts into underground working face and causes property damage and casualties [1]. Some coalfields in North China are covered with thick loose layers, especially in deep mining mines in southwest Shandong Province. When mining near the loose layers, the upper water-rich sand layer is prone to water and sand inrush under the disturbance of mining activities, which affects the normal production of the mine and causes casualties [2, 3]. In order to reduce the occurrence of water and sand inrush disasters and take timely and effective measures, it is necessary to put forward a more accurate assessment method of water and sand inrush disasters under loose layer mining [4, 5].

Experts and scholars studied the problem of water and sand inrush by various methods [6–13]. Zhong et al. used software PFC^{3D} and software GID to simulate the whole process of water and sand inrush in precast ideal fracture with different opening widths and dip angles in overlying rock strata. Their analysis shows that the opening widths and dip angles of fracture change the flow patterns of water-sand flow inrush and have great impact on the contact

force of the fracture channel, flow velocity of water, and the time of mixed water-sand flow [14]. Zhao et al. studied the overlying stratum fracture development and distribution characteristics of water-sand inrush channel through the simulation experiment. They divided the development process of water-inrush channels into three stages: the stage of gradual development, the stage of penetration linking channel formation, and the stage of water-sand inrush, and divided the area of the overlying rock fracture and water-sand inrush into three sections: the zone of overburden fracture gradual development, the zone of water-sand intrusion, and the zone of water-sand-intrusion blocking [15]. Peng et al. made a comprehensive analysis on the mechanism of water and sand inrush disaster from many aspects such as channel, water source, water storage space, power source, and geological structure. They found out that the cause of water and sand inrush disaster under thick overlying bedrock is that the water flowing fractured zone generated by mining causes water to enter the separated cavity between rock formations. The water in the separated cavity penetrates into the loose geological body and breaks into the working face instantly along the concentrated channel generated by cutting the working face, resulting in the occurrence of water and sand inrush disaster [16]. Zhang et al. established the mechanics model of sand inrush in fractures and analyzed the limit equilibrium condition of water and sand inrush in fractures. Through experiments, they quantitatively analyzed the characteristics of water and sand migration and correlation changes of physical parameters in different stages of water and sand inrush and divided the whole process of water and sand inrush in fractures into four stages, namely, start-up stage, continuous outburst stage, silt blockage stage, and outburst equilibrium stage [17]. Ma et al. established a water-sediment flow resistance model in fractures based on the two-phase flow theory and verified it through laboratory-scale test [18]. Using the LBM-DEM coupling simulation method, Pu et al. studied the problem of the water and sand two-phase migration in the single-fracture opening channel model. They compared the changes of section flow rate and sand inrush rate under different boundary pressures, fracture opening widths, and sand layer thickness [19].

As mentioned above, researchers have made many achievements in the mechanism of water and sand inrush. However, the prediction of sudden water and sand inrush is difficult due to the comprehensive influence of many factors, and the influencing factors are fuzzy and random. To solve this problem, a risk assessment method of water and sand inrush is proposed based on comprehensive weight and cloud model in this paper. The membership degree function transformed from the normal cloud generator equation is used to calculate the membership degree of the index. Combine analytic hierarchy process, entropy weight method, and minimum entropy principle to calculate the comprehensive weight of the index. Based on the membership degree and the comprehensive weight, the risk of water and sand inrush of the assessment object is evaluated, hoping it can provide new ideas and methods for the prevention and control of water and sand inrush disasters. The assessment process is shown in Figure 1.

2. Overview of the Study Area

The sixth mining area of Baodian Coal Mine is selected as the study area. The range and location of boreholes near the sixth mining area are shown in Figure 2. Baodian Coal Mine is located in Yanzhou District, Jining City, Shandong Province. The sixth mining area is located in the west of Baodian Coal Mine. The structure is controlled by Yanzhou syncline, and the axial direction is NEE, inclining to the northeast. There is a small south lake syncline in the north of the sixth mining area. The southern development range was Baochang anticline. Fault strike is mostly northeast.

The sixth mining area is a fully concealed North China Carboniferous Permian coalfield. The strata from old to new are Ordovician (O_2), Carboniferous (C), Permian (P), Jurassic (J_3), and Quaternary (Q). The following is a detailed description:

(1) Middle and lower Ordovician ($O_{2,\ 1}$): it is the basement of coal measure strata, which is composed of gray and gray-white limestone

(2) Carboniferous (C): the Taiyuan formation of upper Carboniferous is composed of dark gray-grayish black mudstone, bauxite mudstone, siltstone, and medium-coarse sandstone, with 0-11 layers of limestone. Among them, the thickness of the tenth lower limestone and the third limestone is large and the horizon is stable, which is the auxiliary marker layer of the sixth mining area

(3) Permian (P): Shanxi formation is the main coal-bearing strata in the sixth mining area. It is thick in the north but thin in the south. It is composed of gray-white medium, coarse sandstone, gray siltstone, mudstone, bauxite mudstone, and coal seam. Among them, No. 3 coal seam is the main minable coal seam, which has complete contact with the underlying strata

(4) Jurassic (J_3): the upper member is gray-green, purple-gray medium-fine sandstone. The middle member is loose red sandstone. The next section is brownish-red siltstone. It is distributed within a very small range in the eastern part of the sixth mining area. It is in angular unconformity contact with underlying coal measures

(5) Quaternary (Q): thin in the east and thick in the west, thin in the south, and thick in the north. It is composed of sandy clay, clay sand, clay layer, and medium and coarse sand layers

In all strata, the main coal-bearing area is the Carboniferous strata and Permian strata of Shanxi and Taiyuan formation, which belongs to the type of coal-bearing rock series in North China. The main coal seam is the No. 3 coal seam, with a thickness of about 7.86~10.02 m and an average

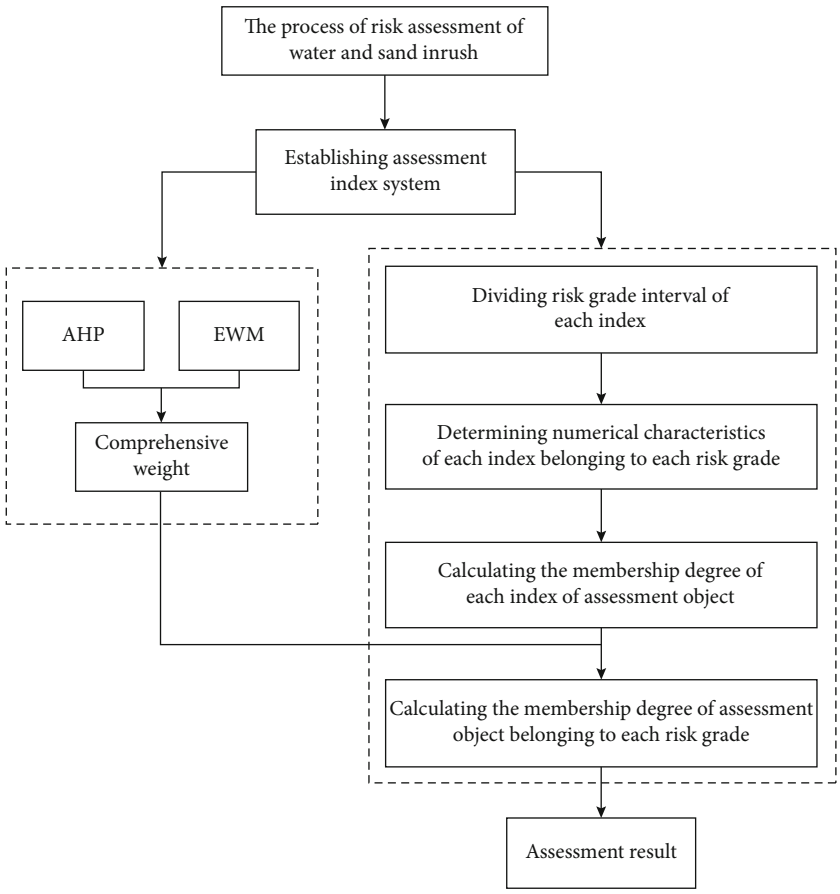

Figure 1: The process of using the comprehensive weight-cloud model method to assess the risk of water and sand inrush during mining under loose layers.

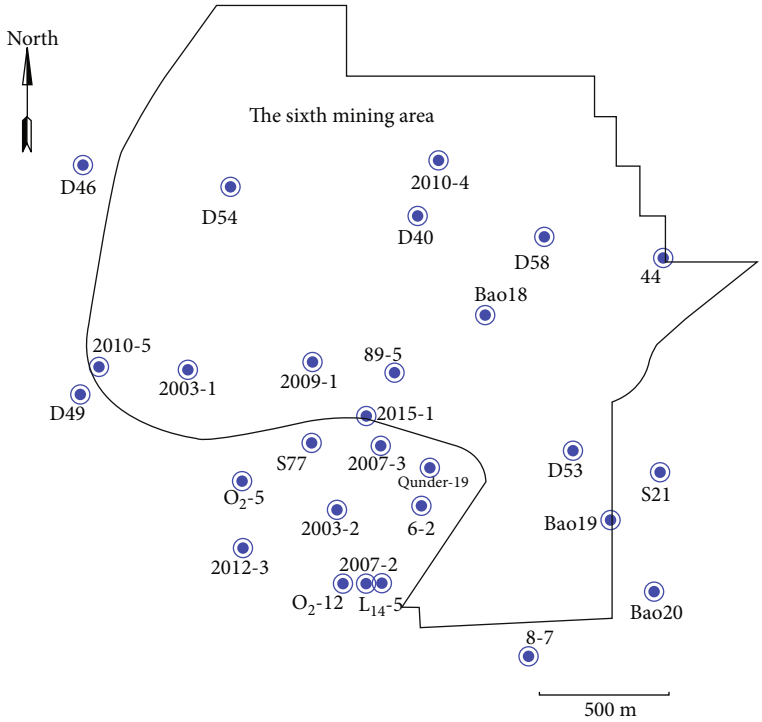

Figure 2: The scope and borehole location of the sixth mining area of Baodian Coal Mine.

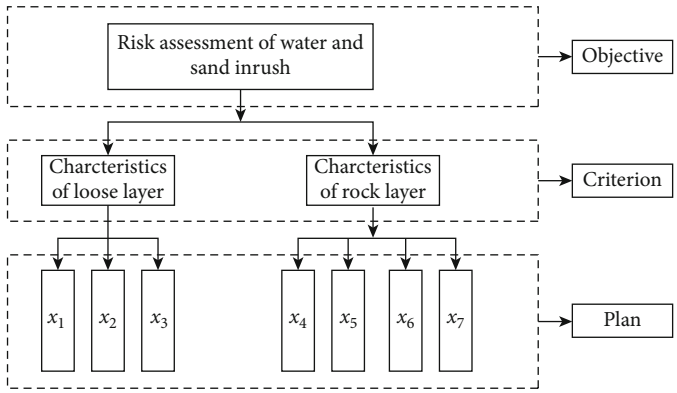

Figure 3: Hierarchical structure system of water and sand inrush index for mining under loose layers.

Table 1: Risk grade interval of water and sand inrush risk assessment index.

Index	Risk grade interval		
	I	II	III
x_1 (m)	0~15	15~30	>30
x_2 (-)	0~1	1~3	>3
x_3 (m)	>10	5~10	0~5
x_4 (m)	0~3.5	3.5~8	>8
x_5 (%)	80~100	60~80	0~60
x_6 (-)	0~0.4	0.4~0.6	0.6~1.0
x_7 (m)	>40	20~40	0~20

thickness of about 9.00 m. The thickness of the coal seam is stable, and the buried depth of coal seam is about 200~390 m.

The main aquifers affecting the production of the No. 3 coal seam in the sixth mining area from top to bottom are the gravel aquifer in the Quaternary upper group, the gravel aquifer in the Quaternary lower group, and the sandstone aquifer at the roof and floor of the No. 3 coal seam. Among them, the direct water-filled aquifer of coal seam mining is the sandstone aquifer at the roof and floor of the No. 3 coal seam and the gravel aquifer in the Quaternary lower group, and the indirect water-filled aquifer is the gravel aquifer in the Quaternary lower group (when the sandstone aquifer at the roof of the No. 3 coal seam is the direct water-filled aquifer). Except for the gravel aquifer in the Quaternary upper group, the remaining aquifers are mainly static reserves, and the recharge, runoff, and discharge conditions are poor. With the development of mining activities, the water level of the sand layer in the Quaternary lower group decreased slowly year by year, and the water level of the sandstone at the roof of the No. 3 coal seam decreased significantly.

3. Assessment Methods

3.1. Analytic Hierarchy Process. American operational researcher Saaty put forward the famous analytic hierarchy process (AHP) in the early 1970s. The analytic hierarchy process is a decision-making method which decomposes the elements related to decision-making into objective, criterion, plan, and other levels and, on this basis, makes qualitative and quantitative analysis [20].

As a weight determination method, the analytic hierarchy process is commonly used in the field of mine water disasters, such as water abundance assessment and floor water inrush risk assessment [21–23]. In this paper, the improved analytic hierarchy process with three scales is used to calculate the weight.

The traditional AHP needs to check the consistency of the judgment matrix. In this paper, the improved three-scale AHP is used for weight calculation, and the traditional AHP is optimized by using the properties of the optimal transfer matrix, so that it naturally satisfies the consistency. It can greatly reduce the number of iterations and make the subjective factors analytic, thereby reducing the system error.

Supposing there are N lower-level indexes under a certain upper-level index, the importance of each index at the same level is compared according to expert consultation, and the comparison matrix $\mathbf{A} = \{a_{ij}\}_{N\times N}$ is established through the following equation:

$$a_{ij} = \begin{cases} -1 & (\text{index } j \text{ is more important than } i), \\ 0 & (\text{index } i \text{ is as important as index } j), \\ 1 & (\text{index } i \text{ is more important than } j), \end{cases} \quad (1)$$

$$t_{ij} = \frac{1}{n}\sum_{k=1}^{N}\left(a_{ik} - a_{jk}\right) = \frac{1}{n}\sum_{k=1}^{N}\left(a_{ik} + a_{kj}\right), \quad (2)$$

$$d_{ij} = \exp\left(t_{ij}\right). \quad (3)$$

Since matrix $\mathbf{A}$ satisfies $a_{ij} = -a_{ji}$ and $a_{ij} = a_{ik} - a_{jk}$, it is an antisymmetric matrix; then, according to the principle of optimal transfer matrix, the optimal transfer matrix $\mathbf{T}$ of matrix $\mathbf{A}$ should conform to Equation (2).

According to the Equations (2) and (3), the judgment matrix $\mathbf{D} = \{d_{ij}\}_{N\times N}$ is obtained.

Due to the properties of the optimal transfer matrix, no consistency check is required. The equation of the weight

Table 2: Index data of boreholes.

Number	Borehole ID	x_1 (m)	x_2 (-)	x_3 (m)	x_4 (m)	x_5 (%)	x_6 (-)	x_7 (m)
1	Q_{under}-19	12.93	4.92	0.00	9.10	83.69	0.30	39.57
2	6-2	15.05	2.10	0.00	9.01	93.15	0.50	10.13
3	Bao19	4.96	1.65	0.00	8.91	94.33	0.30	144.95
4	2015-1	20.00	3.43	0.00	9.01	92.35	0.70	51.36
5	2003-1	26.65	4.76	0.00	8.38	90.50	0.30	66.4
6	2003-2	16.80	11.42	0.00	8.70	71.79	0.10	14.28
7	2010-5	10.99	1.19	0.00	8.10	88.43	0.50	56.66
8	O_2-5	17.37	6.22	3.39	8.02	88.01	0.10	22.68
9	O_2-12	13.80	5.75	0.00	9.00	94.50	0.70	3.57
10	L_{14}-5	13.20	2.73	1.50	8.46	87.42	0.50	70.39
11	2007-2	13.35	3.13	1.39	11.82	87.40	0.90	55.38
12	2007-3	19.26	4.13	0.00	9.16	89.19	0.10	39.65
13	D49	13.50	1.43	1.45	8.60	89.55	0.30	42.83
14	D53	6.5	1.48	4.23	8.39	92.63	0.50	111.89
15	2012-3	34.07	10.88	1.25	2.10	84.84	0.10	2.1
16	89-5	14.15	2.36	10.86	8.07	90.37	0.30	73.4
17	2009-1	41.88	5.88	0.00	5.66	86.48	0.50	19.43
18	2010-4	6.98	1.16	0.00	9.00	90.56	0.30	122.73
19	D40	11.87	1.50	12.15	9.19	91.57	0.30	108.29
20	D46	13.68	1.44	4.12	9.14	88.93	0.30	26.7
21	D54	18.78	4.38	0.00	8.73	89.15	0.10	102.24
22	Bao18	8.05	1.14	0.00	8.84	91.51	0.10	115.9
23	8-7	19.35	2.15	2.00	8.73	86.73	0.10	107.4
24	Bao20	3.82	0.51	0.00	5.87	96.35	0.10	163.93
25	S77	24.20	8.36	2.50	7.70	83.37	0.10	36.73
26	D58	5.14	1.22	2.00	7.96	93.61	0.10	147.29
27	S21	7.80	1.17	3.75	9.46	97.38	0.10	152.34
28	44	8.20	3.24	1.95	9.03	92.34	0.10	171.18

Table 3: Weights determined by the analytic hierarchy process, the entropy weight method, and the comprehensive weight method.

Weight vector	x_1	x_2	x_3	x_4	x_5	x_6	x_7
$\mathbf{W}_1$	0.1513	0.0399	0.0777	0.2018	0.1224	0.0742	0.3327
$\mathbf{W}_2$	0.1362	0.1311	0.1730	0.1649	0.1092	0.1332	0.1524
$\mathbf{W}_3$	0.1504	0.0758	0.1215	0.1911	0.1211	0.1042	0.2359

w_i of the index i is as follows:

$$w_i = \frac{\sqrt[N]{\prod_{j=1}^{N} d_{ij}}}{\sum_{i=1}^{N}\left(\sqrt[N]{\prod_{j=1}^{N} d_{ij}}\right)} \quad (i = 1, 2, \cdots, N). \tag{4}$$

Finally, according to Equation (4), the weight of the plan level to the criterion level and the weight of the criterion level to the objective level are calculated, respectively, and then, the weight vector $\mathbf{W}_1 = \{w_{1i}\}_{1\times n}$ of the plan level to the objective level is obtained, where n is the index number in the plan level.

3.2. Entropy Weight Method. As a weight calculation method, entropy weight method (EWM) has been well applied in the weight calculation of multifactor indexes [24–27].

Assuming that there are m samples and each sample has n indexes, the original matrix $\mathbf{R} = \{R_{ij}\}_{m\times n}$ can be constructed, where R_{ij} represents the data of index j of the sample i.

Then, according to the original matrix $\mathbf{R}$, the normalized matrix $\mathbf{r} = \{r_{ij}\}_{m\times n}$ is calculated.

For the positive indexes that the greater the better indexes, the calculation equation is as follows:

$$r_{ij} = \frac{R_{ij} - \min\{R_{1j}, R_{2j}, \cdots, R_{mj}\}}{\max\{R_{1j}, R_{2j}, \cdots, R_{mj}\} - \min\{R_{1j}, R_{2j}, \cdots, R_{mj}\}}. \tag{5}$$

For negative indexes that the smaller the better indexes, the calculation equation is as follows:

$$r_{ij} = \frac{\max\{R_{1j}, R_{2j}, \cdots, R_{mj}\} - R_{ij}}{\max\{R_{1j}, R_{2j}, \cdots, R_{mj}\} - \min\{R_{1j}, R_{2j}, \cdots, R_{mj}\}}. \tag{6}$$

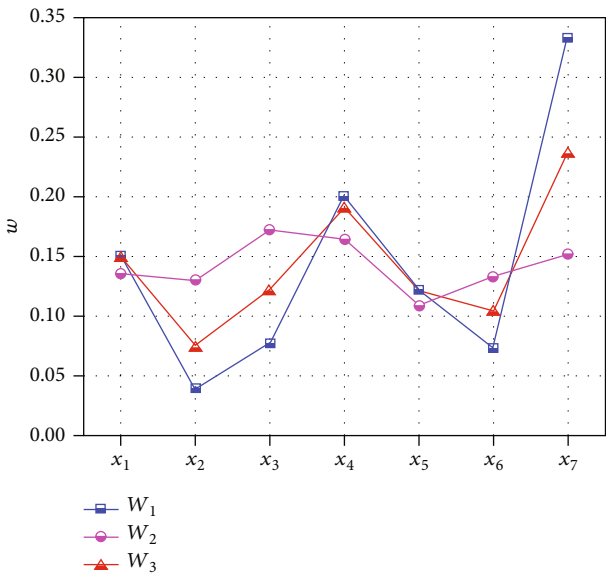

Figure 4: Comparison of weights determined by the analytic hierarchy process, the entropy weight method, and the comprehensive weight method.

Table 4: Numerical characteristics of each index belonging to each risk grade.

Index	Numerical characteristics		
	I	II	III
x_1	(7.5, 6.369, 0.5)	(22.5, 6.369, 0.5)	(37.5, 6.369, 0.5)
x_2	(0.5, 0.425, 0.05)	(2, 0.849, 0.05)	(9.5, 5.520, 0.05)
x_3	(12.5, 2.123, 0.2)	(7.5, 2.123, 0.2)	(2.5, 2.123, 0.2)
x_4	(1.75, 1.486, 0.1)	(5.75, 1.911, 0.1)	(10, 1.699, 0.1)
x_5	(90, 8.493, 1)	(70, 8.493, 1)	(30, 25.478, 1)
x_6	(0.2, 0.170, 0.001)	(0.5, 0.085, 0.001)	(0.8, 0.170, 0.001)
x_7	(108, 57.325, 1)	(30, 8.493, 1)	(10, 8.493, 1)

According the normalized matrix $\mathbf{r} = \{r_{ij}\}_{m\times n}$, calculate the proportion p_{ij} of the j index data of the i sample:

$$p_{ij} = \frac{1 + r_{ij}}{\sum_{j=1}^{n}(1 + r_{ij})}. \tag{7}$$

Then, calculate the entropy of all index, and the calculation equation for the entropy value H_j of the index j is

$$H_j = \frac{\sum_{j=1}^{m} p_{ij} \ln p_{ij}}{\ln m}. \tag{8}$$

Calculate the entropy weight of all index, and the calculation equation for the entropy weight w_j of the index j is

$$w_j = \frac{1 - H_j}{\sum_{j=1}^{n}(1 - H_j)}. \tag{9}$$

Finally, get the weight vector $\mathbf{W}_2 = \{w_{2i}\}_{1\times n}$.

3.3. Comprehensive Weight. Each weight calculation method has its own scope of application, and sometimes, it is often necessary to use a variety of methods to measure the weight of the same data, so that the comprehensive weight has higher performance and can reflect the real characteristics of the data. According to the minimum entropy principle, this paper processes the weight vector $\mathbf{W}_1$ determined by the analytic hierarchy process and the weight vector $\mathbf{W}_2$ determined by the entropy weight method to determine the comprehensive weight vector $\mathbf{W}_3$ [28, 29]. The calculation process is as follows:

$$w_{3j} = \frac{\sqrt{w_{1j} \times w_{2j}}}{\sum_{j}^{n} \sqrt{w_{1j} \times w_{2j}}}, \tag{10}$$

$$\mathbf{W}_3 = (w_{31} w_{32} \cdots w_{3n}). \tag{11}$$

3.4. Cloud Model. Cloud model is an uncertain cognitive model based on fuzzy set theory and probability concept, which was proposed by Liu et al. [27]. The cloud model can be used to deal with the uncertain conversion between qualitative concepts and quantitative description and has been widely used in algorithm improvement, simulation, risk assessment, geological prediction, excavation, and other fields [30–33]. In the conversion process from quantitative data (influencing factors data) to qualitative concepts (risk grade), the cloud model can better handle the effects of randomness and ambiguity, thus making the evaluation results more scientific and accurate.

Normal cloud is an important cloud model based on normal distribution and Gaussian membership function. Since the expected value curves of influencing factors in natural science are mostly normal distribution or seminormal distribution [34], the normal cloud model is used in this paper to evaluate the risk of water and sand inrush.

Supposing the set $X = \{x\}$ is a domain, the qualitative concept on the domain is defined as Y. For any x belonging to X, there exists a random number $u(x)$ belonging to Y. The set of $u(x)$ is called the membership degree of x belonging to Y, if $u(x)$ satisfies

$$u(x) = \exp\left(-\frac{(x - \mathrm{Ex})^2}{2\mathrm{En}'2}\right). \tag{12}$$

If x satisfies $x \sim N(\mathrm{Ex}, \mathrm{En}'2)$ and $\mathrm{En}' \sim N(\mathrm{En}, \mathrm{He}^2)$, the distribution of x on X is called a normal cloud, and each x is called a cloud drop. Ex, En, and He are the numerical characteristics of a qualitative concept, where Ex represents expectation, En represents entropy, and He represents hyperentropy. If the three numerical characteristics of the qualitative concept are known, the normal cloud generator can be used to generate the normal cloud. The process is as follows:

Step 1. Generate a normal random number En' with an expected value of En and a standard deviation of He.

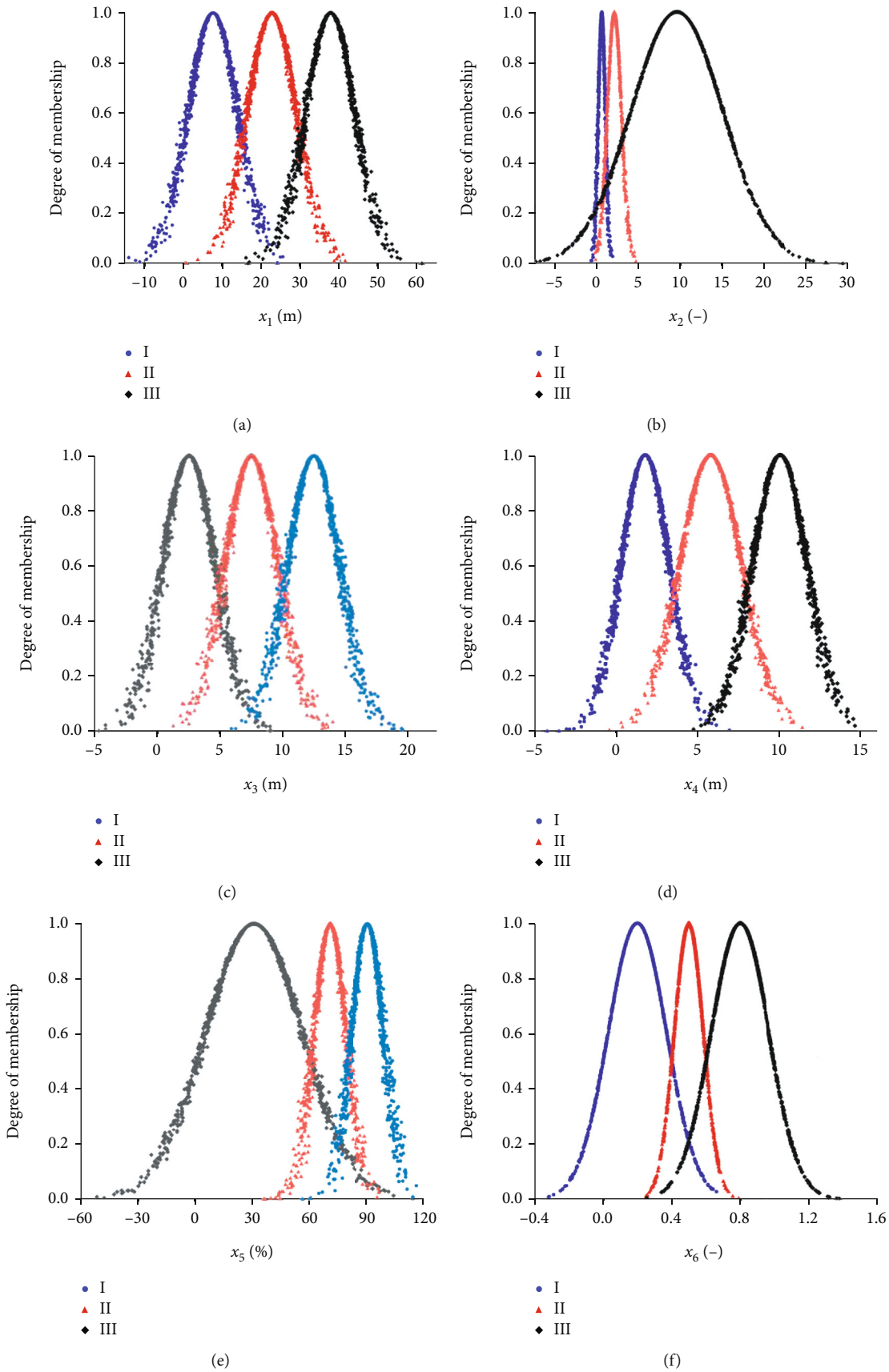

Figure 5: Continued.

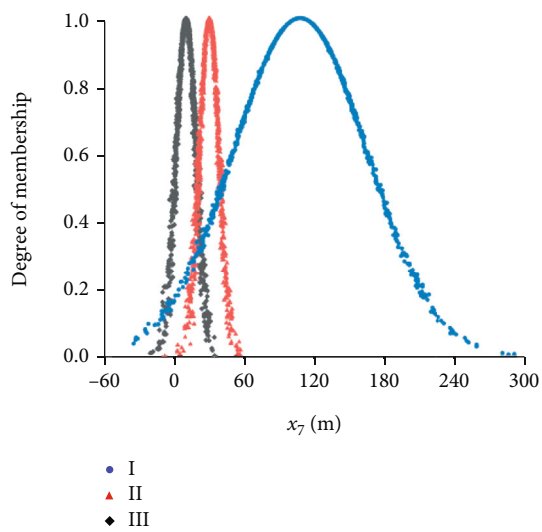

(g)

Figure 5: Normal cloud of each index belonging to each risk grade.

Table 5: Working face index data.

Name of working face	x_1 (m)	x_2 (-)	x_3 (m)	x_4 (m)	x_5 (%)	x_6 (-)	x_7 (m)
6311-2	26.90	3.81	0.00	8.64	89.15	0.30	53.51

Table 6: Membership degree of working face belonging to each risk grade.

Name of working face	Membership degree			Comprehensive weight-cloud model	Actual situation
	I	II	III		
6311-2	0.3610	0.2086	0.2912	I	I

Step 2. Generate a normal random number x with an expected value of Ex and a standard deviation of abs(En').

Step 3. Calculate $u(x)$ through Equation (12), and a cloud drop x with a membership degree of $u(x)$ for the qualitative concept is generated.

Step 4. Repeat Step 1–Step 3 until the number of cloud drops meets the requirements.

The calculation of the numerical characteristics (Ex_{ij}, En_{ij}, and He_{ij}) and of the index i belonging to the risk grade j is as follows.

Assuming that the upper and lower boundary values of the index i belonging to the risk grade j are x_{ij}^1 and x_{ij}^2, then

$$\mathrm{Ex}_{ij} = \frac{\left(x_{ij}^1 + x_{ij}^2\right)}{2}. \tag{13}$$

Since the boundary value is from one grade to another and should belong to both grades [32], so

$$\mathrm{En}_{ij} = \frac{\left(x_{ij}^1 - x_{ij}^2\right)}{2.355}. \tag{14}$$

The size of He_{ij} is determined according to the fuzziness and randomness of the specific case, and the value is about 0.1 times of En_{ij} [35].

Some scholars use the cloud model to obtain the membership degree by using the cloud generator to randomly generate cloud drops and then obtain the average membership degree [33]. The membership degree obtained by this method has a certain degree of volatility, resulting in the same calculation process which may not be able to obtain the same assessment results. In order to obtain a stable membership degree, the membership function is obtained based on Equation (12). The membership function is shown below:

$$u_{ij} = \exp\left(-\frac{\left(x_i - \mathrm{Ex}_{ij}\right)^2}{2\mathrm{En}_{ij}}\right), \tag{15}$$

where x_i represents the value of the index i and u_{ij} represents the membership degree of the index i belonging to the risk grade j.

The membership degree matrix $\mathbf{U} = \{u_{ij}\}_{n\times l}$ of the assessment object is obtained, where n is the number of indexes, and l is the number of risk grades.

In order to find out the membership degree of the assessment object to a risk grade, it is necessary to multiply the membership degree of index of the assessment object corresponding to the risk grade by the index weight and add

them, so as to obtain the membership degree of the assessment object to the risk grade.

The comprehensive weight vector $\mathbf{W}_3$ is combined with the membership matrix $\mathbf{U}$ of the assessment object to obtain the matrix $\mathbf{B}$.

$$\mathbf{B} = \mathbf{W}_3\mathbf{U} = (b_1, b_2, \cdots, b_n), \tag{16}$$

$$b_j = \sum_{i=1}^{n} w_i u_{ij} \quad (j = 1, 2, \cdots, l). \tag{17}$$

In Equation (17), b_j represents the membership of the assessment object to the risk grade j. Then, according to the principle of maximum membership degree, the risk grade $j_{\max}$ corresponding to the maximum membership degree $b_{j\ \max}$ is the water inrush risk grade of the assessment object.

4. Preparation of Assessment

4.1. Index Selection. The occurrence of water and sand inrush in the mining under the loose layer depends on the combined effect of various influencing factors. According to the hydrogeological data in the sixth mining area of Baodian Coal Mine, this paper selects seven influencing factors, namely, the aquifer thickness (x_1), the thickness ratio of the sand layer to clay layer (x_2), the thickness of the bottom clay layer (x_3), the coal seam thickness (x_4), the percentage of core recovery (x_5), the geological structure (x_6), and the bedrock thickness (x_7), as index. These factors can be categorized into the characteristics of loose layer and the characteristics of rock layer. The hierarchical structure system of water and sand inrush index for mining under loose layer in the mining under the loose layer is shown in Figure 3.

(1) The aquifer thickness (x_1). Generally speaking, the aquifer in the loose layer is mainly sand layer. Thicker aquifer can store more groundwater, and under the influence of mining, there is a greater possibility of water and sand inrush [36]

(2) The thickness ratio of the sand layer to clay layer (x_2). The sand layer with fractures has strong water storage and water conductivity, while the clay layer has certain water and sand resistance. The thickness ratio of the sand layer to clay layer in the loose layer of the Quaternary lower group determines the risk of water and sand inrush

(3) The thickness of the bottom clay layer (x_3). The clay layer at the bottom of the loose layer is a powerful barrier that directly hinders the downward seepage and inrush of water and sand in the upper aquifer. The thicker the clay layer at the bottom is, the more likely it will reduce the possibility of water and sand inrush in the exploitation of coal resources [36]

(4) The coal seam thickness (x_4). The height of the roof fall zone and fracture zone caused by coal seam mining is related to the cumulative mining thickness of the coal seam. Generally speaking, the greater the cumulative mining thickness of the coal seam, the greater the height of the caving zone and fracture zone of the roof. In mining, it is necessary to set sand-prevention coal and rock pillars to avoid excessive water and sand inrush due to the excessive height of the caving zone and fracture zone. Since No. 3 coal is the main mineable coal seam in the sixth mining area, this paper uses the thickness of the No. 3 coal seam instead of the cumulative mining thickness as the index [37]

(5) The percentage of core recovery (x_5). The integrity of the core taken during drilling is related to the degree of rock fragmentation. The core of the bedrock is relatively complete, indicating that the bedrock has a low degree of fragmentation and is an effective water-blocking layer. The possibility of water and sand inrush is low when mining [38]

(6) The geological structure (x_6). The development degree of geological structure can be expressed by density of faults, fault drop, density of joints, etc. The area with developed geological structures has high risk of water and sand inrush. Based on the actual mining experience and geological data, the degree of geological structure development is divided, and the equation is as follows [39]:

$$x_6 = \begin{cases} 0.1, & \text{not developed,} \\ 0.3, & \text{less developed,} \\ 0.5, & \text{more developed,} \\ 0.7, & \text{developed,} \\ 0.9, & \text{very developed.} \end{cases} \tag{18}$$

(7) The bedrock thickness (x_7). The bedrock is thick and stable, the fracture zone cannot develop to the aquifer, and the risk of water and sand inrush is low. If the bedrock is thin or missing, the fracture zone develops to the aquifer, and the risk of water and sand inrush is high [33, 40]

4.2. Risk Grade. The risk of water and sand inrush is divided into three grades, namely, low risk (I), medium risk (II), and high risk (III). The corresponding situation of grade I is that the aquifer at the bottom of the loose layer has little influence on the mining of the working face, and the water and sand inrush will not occur in the mining process. The corresponding situation of grade II is that the aquifer at the bottom of the loose layer has a certain influence on the mining of the working face. For example, the roof of the working face often shows the phenomenon of water leaching, and the water inflow of the working face changes greatly; mining process, sudden water, and sand inrush

may occur. The corresponding situation of grade III is that the aquifer at the bottom of the loose layer has a great impact on the mining of the working face. When the roof comes to pressure, the water inflow of the working face changes greatly, and there is a great possibility of sudden water and sand inrush in the mining process. According to the engineering experience, each index is divided into intervals according to the risk grade, as shown in Table 1.

4.3. Weight Calculation. Based on the analysis and statistics of hydrogeological data and borehole data in the study area, 28 borehole data are collected as samples, as shown in Table 2, and the borehole locations are shown in Figure 2.

After consulting and analysis, this paper argues that for the occurrence of water and sand inrush, in the criterion level, the characteristics of the rock layer are greater than the characteristics of loose layer. For the characteristics of loose layer, the index weights in descending order are the aquifer thickness (x_1), the thickness of the bottom clay layer (x_3), and the thickness ratio of the sand layer to clay layer (x_2). For the characteristics of the rock layer, the index weights in descending order are the bedrock thickness (x_7), the coal seam thickness (x_4), the percentage of core recovery (x_5), and the geological structure (x_6). The comparison matrix $\mathbf{A}_1$ of criterion level and the comparison matrices $\mathbf{A}_2$ and $\mathbf{A}_3$ of plan level are obtained as follows:

$$\mathbf{A}_1 = \begin{bmatrix} 0 & -1 \\ 1 & 0 \end{bmatrix},$$
$$\mathbf{A}_2 = \begin{bmatrix} 0 & 1 & 1 \\ -1 & 0 & -1 \\ -1 & 1 & 0 \end{bmatrix}, \tag{19}$$
$$\mathbf{A}_3 = \begin{bmatrix} 0 & 1 & 1 & -1 \\ -1 & 0 & 1 & -1 \\ -1 & -1 & 0 & -1 \\ 1 & 1 & 1 & 0 \end{bmatrix}.$$

The weight vector $\mathbf{W}_1$ is calculated according to Equation (4). According to the data in Table 2, the weight vector $\mathbf{W}_2$ is determined by the entropy weight method, and then, the comprehensive weight vector $\mathbf{W}_3$ is obtained by Equation (10). Analyzing the weight vector $\mathbf{W}_2$, the thickness of the bottom clay layer (x_3), the coal seam thickness (x_4), and the bedrock thickness (x_7) have a greater impact on the risk of water and sand inrush. Among the weight vector $\mathbf{W}_3$, the aquifer thickness (x_1), the coal seam thickness (x_4), and the bedrock thickness (x_7) are larger. Combining the weights determined by the three methods, it can be concluded that the coal seam thickness (x_4) and the bedrock thickness (x_7) are the main influencing factors of water and sand inrush. The index weights of the three methods are shown in Table 3 and Figure 4.

4.4. Numerical Characteristics. Based on the risk grade range and borehole sample data (Table 2), by using Equations (13) and (14), the numerical characteristics (Ex, En, and He) of each index belonging to risk grades I, II, and III are determined, as shown in Table 4.

According to the normal cloud generation process and the numerical characteristics, the normal cloud of each index belonging to each risk grade is generated (Figure 5). The number of the cloud drops for each normal cloud is 1000. The normal cloud can represent the distribution of the membership degree of the index belonging to a certain risk grade.

As can be seen from Figure 5, Ex determines the position of the center point of the risk grade normal cloud; En determines the range of the risk grade normal cloud. The larger the En, the larger the risk level normal cloud range. He determines the discreteness of the normal cloud of risk grades. When the ratio of He to En is small, the distribution of the normal cloud tends to a curve with a normal distribution. When the ratio of He to En is large, the dispersion of the normal cloud is large.

5. Verification via the Application

The 6311-2 working face is located in the west of Baodian Coal Mine, and the south of the working face is close to the outcrop area of the No. 3 coal seam aeolian oxidation zone in the sixth mining area. The No. 3 coal seam is mined at the working face, the thickness of the coal seam is about 8.12~9.16 m, and the average is about 8.64 m. The Quaternary lower group is composed of gray-green, gray-yellow, and gray-white clay; clay-bearing gravel; and sand. The main aquifers of the lower group are clay gravel and gravel layers.

The coal seam of the working face is a monoclinic structure and belongs to the north wing of the Baojiachang anticline. Small secondary wide and gentle folds are developed in the working face. The maximum water inflow of the 6311-2 working face during mining is 24 m^3/h, and it is 18.9 m^3/h under normal conditions. The water inflow of the working face is basically the water inflow after mining and the water inflow during production. The working face did not show excessive water inrush locally and at intervals, and no water and sand inrush disaster occurred.

According to the corresponding geological report, the index data of the working face was determined (Table 5), by using Equations (15)–(17) to calculate the membership degree of the working face belonging to each risk grade according to the index data of the working face. According to the calculation results (Table 6), the maximum membership degree of the 6311-2 working face is 0.3610, and the water and sand inrush risk grade corresponding to the maximum membership degree is grade I, which means that water and sand inrush will not occur in mining. The actual mining process of this working face did not appear to have water and sand inrush, which is consistent with the prediction of the comprehensive weight-cloud model assessment method proposed in this paper. This result illustrates the feasibility of this method.

6. Conclusions

To reduce the randomness and ambiguity of the influencing factors in the prediction of the risk of water and sand inrush and to better assess the risk of water and sand inrush in short-distance mining under thick loose layers of coal mines, this paper proposes a new risk assessment method of water and sand inrush based on the comprehensive weight and cloud model. The method is applied to the risk assessment of water and sand inrush in the 6311-2 working face in the sixth mining area of Baodian Coal Mine. The following conclusions are drawn from the research:

(1) Analyzing the weights determined by the analytic hierarchy process, the entropy weighting method, and the comprehensive weighting method, the weight of the bedrock thickness and the coal seam thickness are all ranked in the top three of the three weights. It can be considered that among the seven indicators that affect the risk of water inrush and sand inrush, the bedrock thickness and the coal seam thickness have a greater influence on the risk of water inrush and sand inrush and are the main influencing factors

(2) The comprehensive weight-cloud model method is applied to assess the risk of water and sand inrush in the working face, and the assessment result is consistent with the actual situation. It shows that the comprehensive weight-cloud model method has good prediction performance and can provide scientific reference for safe mining under thick loose layer in deep mines in southwest Shandong

(3) The comprehensive weight-cloud model method is based on the existing sample data. The number of samples, the selection of indexes, and the division of risk grade interval will have a certain impact on the assessment results of the method. In view of the complexity of water and sand inrush in close-distance mining under thick loose layer, in order to obtain more accurate prediction results, it is necessary to collect more engineering examples and sample data, so as to improve the accuracy of the method

Data Availability

All data, models, or codes generated or used during the study are available from the corresponding author by request.

Conflicts of Interest

The authors declare no conflicts of interest.

Acknowledgments

The authors of the paper would like to extend grateful thanks to the National Natural Science Foundation of China (Grant No. 51774199) for its support and Baodian Coal Mine for providing relevant geological data.

References

[1] W. H. Sui, Y. K. Liang, G. L. Zhang, Q. H. Dong, and B. B. Yang, "Study status and outlook of risk evaluation on water inrush and sand inrush mechanism of excavation and mining," *Coal Science and Technology*, vol. 39, no. 11, pp. 5–9, 2011.

[2] Z. H. Li, X. P. Ding, and Z. H. Cheng, "Research on fractal characteristics of overlying strata crack evolution in coal seam with thin bedrock," *Journal of Mining & Safety Engineering*, vol. 27, no. 4, pp. 576–580, 2010.

[3] W. H. Sui, D. D. Wang, Y. J. Sun, W. F. Yang, Z. M. Xu, and L. Feng, "Mine hydrogeological structure and its responses to mining," *Journal of Engineering Geology*, vol. 27, no. 1, pp. 21–28, 2019.

[4] H. Q. Lian, X. X. Xia, W. Ran, and T. Yan, "Possibility analysis of water and sand inrush at shallow buried coal seam with unconsolidated formation and thin bedrock," *Safety in Coal Mines*, vol. 46, no. 2, pp. 168–171, 2015.

[5] F. Wang, C. Zhang, X. Zhang, and Q. Song, "Overlying strata movement rules and safety mining technology for the shallow depth seam proximity beneath a room mining goaf," *International Journal of Mining Science and Technology*, vol. 25, no. 1, pp. 139–143, 2015.

[6] B. Chen, S. C. Zhang, Y. Y. Li, and J. P. Li, "Experimental study on water and sand inrush of mining cracks in loose layers with different clay contents," *Bulletin of Engineering Geology and the Environment*, vol. 80, no. 1, pp. 663–678, 2021.

[7] G. Fan, D. Zhang, S. Zhang, and C. Zhang, "Assessment and prevention of water and sand inrush associated with coal mining under a water-filled buried gully: a case study," *Mine Water and the Environment*, vol. 37, no. 3, pp. 565–576, 2018.

[8] H. Li, J. Li, L. Li, H. Xu, and J. Wei, "Prevention of water and sand inrush during mining of extremely thick coal seams under unconsolidated Cenozoic alluvium," *Bulletin of Engineering Geology and the Environment*, vol. 79, no. 6, pp. 3271–3283, 2020.

[9] Q. Liu and B. Liu, "Experiment study of the failure mechanism and evolution characteristics of water-sand inrush geo-hazards," *Applied Sciences*, vol. 10, no. 10, p. 3374, 2020.

[10] Y. Xu, Y. Luo, J. Li, K. Li, and X. Cao, "Water and sand inrush during mining under thick unconsolidated layers and thin bedrock in the Zhaogu No. 1 Coal Mine, China," *Mine Water and the Environment*, vol. 37, no. 2, pp. 336–345, 2018.

[11] W. Yang, L. Jin, and X. Zhang, "Simulation test on mixed water and sand inrush disaster induced by mining under the thin bedrock," *Journal of Loss Prevention in the Process Industries*, vol. 57, pp. 1–6, 2019.

[12] D. Ma, H. Duan, X. Li, Z. Li, Z. Zhou, and T. Li, "Effects of seepage-induced erosion on nonlinear hydraulic properties of broken red sandstones," *Tunnelling and Underground Space Technology*, vol. 91, article 102993, 2019.

[13] D. Ma, H. Duan, J. Zhang, X. Feng, and Y. Huang, "Experimental investigation of creep-erosion coupling mechanical properties of water inrush hazards in fault fracture rock masses," *Chinese Journal of Rock Mechanics and Engineering*, vol. 40, no. 9, pp. 1751–1763, 2021.

[14] J. C. Zhong, H. W. Zhou, Y. F. Zhao, Y. Q. Liu, H. Y. Yi, and D. J. Xue, "The two-phase flow of water-sand inrush under shallow coal seam mining: a coupled numerical study," *Engineering Mechanics*, vol. 34, no. 12, pp. 229–238, 2017.

[15] Q. F. Zhao, N. Zhang, C. L. Han et al., "Simulation experiment of water-sand inrush during the mining of the shallow coal seam under roof aquifer with thin bedrock," *Journal of Mining & Safety Engineering*, vol. 34, no. 3, pp. 444–451, 2017.

[16] T. Peng, X. H. Feng, L. L. Long, Y. Wang, C. Niu, and Y. F. Liu, "Study on mechanism of water inrush and sand inrush in mining of coal seam with thick overlying bedrock," *Coal Science and Technology*, vol. 47, no. 7, pp. 260–264, 2019.

[17] S. C. Zhang, Y. Y. Li, J. P. Li, W. H. Yang, G. L. Wang, and Z. J. Wen, "Experimental studies on variation characteristics of physical parameters during water and sand burst through mining fractures," *Journal of China Coal Society*, vol. 45, no. 10, pp. 3548–3555, 2020.

[18] D. Ma, H. Duan, W. Liu, X. Ma, and M. Tao, "Water–sediment two-phase flow inrush hazard in rock fractures of overburden strata during coal mining," *Mine Water and the Environment*, vol. 39, no. 2, pp. 308–319, 2020.

[19] H. Pu, S. R. Guo, D. J. Liu, J. C. Xu, and J. Wang, "Study on laws of water inrush and sand burst migration based on LBM-DEM coupling method," *Coal Science and Technology*, vol. 49, no. 2, pp. 206–216, 2021.

[20] X. Deng, J. M. Li, H. J. Zeng, J. Y. Chen, and J. F. Zhao, "Analysis and application research on the weight calculation method of AHP," *Mathematics in Practice and Theory*, vol. 42, no. 7, pp. 93–100, 2012.

[21] Y. S. Bi, J. W. Wu, X. R. Zhai, S. H. Shen, R. Hu, and Q. D. Ju, "Evaluation of coal mine aquifer water-richness based on AHP and independent weight coefficient method," *Journal of China Hydrology*, vol. 40, no. 4, pp. 40–45, 2020.

[22] Q. Li and W. H. Sui, "Risk evaluation of mine-water inrush based on principal component logistic regression analysis and an improved analytic hierarchy process," *Hydrogeology Journal*, vol. 29, no. 3, pp. 1299–1311, 2021.

[23] J. X. Wang, H. S. Liu, and M. Qiu, "FDAHP-TOPSIS model for evaluation of the water inrush risk from coal floors," *Journal of Mining and Strata Control Engineering*, vol. 3, no. 2, pp. 104–115, 2021.

[24] X. Y. Fan, Z. X. Jia, X. L. Bai, T. J. Yang, and Y. Liu, "Classification of extremely soft rock tunnels using comprehensive evaluation model of entropy-weighted fuzzy," *Journal of Engineering Geology*, vol. 27, no. 6, pp. 1236–1243, 2019.

[25] X. B. Gu, S. T. Wu, X. Ji, and Y. H. Zhu, "The risk assessment of debris flow hazards in Banshanmen gully based on the entropy weight-normal cloud method," *Advances in Civil Engineering*, vol. 2021, Article ID 8841310, 11 pages, 2021.

[26] J. Y. Li, Q. M. Liu, Y. Liu, and H. C. Chai, "Risk assessment of water inrush from coal seam roof based on GIS and entropy method," *Coal Engineering*, vol. 51, no. 8, pp. 115–119, 2019.

[27] W. T. Liu, Q. Sun, and B. C. Xu, "Risk evaluation of water inrush from coal seam floor based on GIS and principal component analysis-entropy weight method," *Mining Research and Development*, vol. 40, no. 11, pp. 83–88, 2020.

[28] W. Q. Zhang, Z. Y. Wang, J. L. Shao, X. X. Zhu, W. Li, and X. T. Wu, "Evaluation on the stability of vertical mine shafts below thick loose strata based on the comprehensive weight method and a fuzzy matter-element analysis model," *Geofluids*, vol. 2019, Article ID 3543957, 15 pages, 2019.

[29] H. Bai, F. Feng, J. Wang, and T. Wu, "A combination prediction model of long-term ionospheric foF2 based on entropy weight method," *Entropy*, vol. 22, no. 4, p. 442, 2020.

[30] D. Y. Li, H. J. Meng, and X. M. Shi, "Membership cloud and membership cloud generator," *Journal of Computer Research and Development*, vol. 32, no. 6, pp. 15–20, 1995.

[31] X. T. Wang, S. C. Li, X. Y. Ma, Y. G. Xue, J. Hu, and Z. Q. Li, "Risk assessment of rockfall hazards in a tunnel portal section based on normal cloud model," *Polish Journal of Environmental Studies*, vol. 26, no. 5, pp. 2295–2306, 2017.

[32] K. G. Li, M. L. Li, and Q. C. Qin, "Research on evaluation method of rock burst tendency based on improved comprehensive weighting," *Chinese Journal of Rock Mechanics and Engineering*, vol. 39, no. S1, pp. 2751–2762, 2020.

[33] X. T. Wang, S. C. Li, Z. H. Xu, J. Hu, D. D. Pan, and Y. G. Xue, "Risk assessment of water inrush in karst tunnels excavation based on normal cloud model," *Bulletin of Engineering Geology and the Environment*, vol. 78, no. 5, pp. 3783–3798, 2019.

[34] X. J. Chen, L. J. Chen, Y. Song, and P. Y. Bi, "Prediction and analysis of karst collapse with entropy-normal cloud model," *Journal of Engineering Geology*, vol. 27, no. 6, pp. 1389–1394, 2019.

[35] Z. Y. Chen and Z. H. Dai, "Improved cloud model for stability evaluation of reservoir slopes," *Journal of Engineering Geology*, vol. 28, no. 3, pp. 619–625, 2020.

[36] W. Zhang, Z. Wang, X. Zhu, W. Li, B. Gao, and H. Yu, "A risk assessment of a water-sand inrush during coal mining under a loose aquifer based on a factor analysis and the Fisher model," *Journal of Hydrologic Engineering*, vol. 25, no. 8, 2020.

[37] W. T. Liu, J. X. Li, and W. Q. Zhang, "Fuzzy mathematical method for roof water inflow grade evaluation," *Journal of China Coal Society*, vol. 26, no. 4, pp. 399–403, 2001.

[38] Y. D. Ji, "The risk assessment of roof water inrush based on cluster analysis and fuzzy comprehensive evaluation," *Mining Safety & Environmental Protection*, vol. 46, no. 4, pp. 68–72, 2019.

[39] W. Q. Zhang, G. P. Zhang, W. Li, and X. Hu, "A model of Fisher's discriminant analysis for evaluating water inrush risk from coal seam floor," *Journal of China Coal Society*, vol. 38, no. 10, pp. 1831–1836, 2013.

[40] B. Li, W. Q. Zhang, and L. Ma, "Influencing factors and prediction of mine water inrush disaster under thick unconsolidated layers and thin bedrock," *Journal of Shandong University of Science and Technology (Natural Science)*, vol. 36, no. 6, pp. 39–46, 2017.